

Ultrarelativistic electron bunches of solid densities and nuclear radiation from nanolayers-plasma-targets under superintense laser pulses

H.K. Avetissian¹, H.H. Matevosyan², G.F. Mkrtchian¹, and Kh.V. Sedrakian¹

¹ *Centre of Strong Fields Physics, Yerevan State University, 1 A. Manukian, Yerevan 0025, Armenia and*

² *Plasma Theory Group, Institute of Radiophysics and Electronics, 0203 Ashtarak, Armenia*

(Dated: March 5, 2022)

We consider nonlinear interaction of superpower laser pulses of relativistic intensities with nanolayers and solid-plasma-targets towards the production of high energy-density electron bunches along with nuclear radiation (hard γ -quanta and positron fluxes). It is shown that petawatt lasers are capable of producing via two-target scheme high density field-free electron/positron bunches and substantial amounts of γ -quanta with energies up to 200 MeV. For actual supershort and tightly focused—strongly nonplane ultrarelativistic laser pulses of linear and circular polarizations 3D3V problem is solved via numerical simulations.

PACS numbers: 41.75.Jv, 41.75.Ht, 52.38.Ph

I. INTRODUCTION

Acceleration of electrons with superpower laser beams (at present –of relativistic intensities) and their interaction with the matter in ultrashort space-time scales have attracted broad interest over the last two decades, stimulated by the continued progress made in laser technology. In many laboratories [1–4] compact lasers can deliver 1 – 10 petawatt short pulses, with focused intensities as high as 10^{22} W cm⁻². Next generation multipetawatt and exawatt optical laser systems [5–7] will be capable to deliver ultrahigh intensities exceeding 10^{25} W cm⁻², which are well above the ultrarelativistic regime of electron-laser interaction. Laser intensities at which an electron becomes relativistic is defined by the condition $\xi \gtrsim 1$, where $\xi = eE\lambda/mc^2$ is the relativistic invariant dimensionless parameter of a wave-particle interaction (e is the elementary charge, c is the light speed in vacuum, and m is the electron mass) and represents the work of the wave electric field with strength E on a wavelength λ ($\lambda = \lambda/2\pi$) in the units of electron rest energy. Laser intensities expressed via ξ can be estimated as:

$$I_r = \xi^2 \times 1.37 \times 10^{18} \text{ W cm}^{-2} [\lambda/\mu\text{m}]^{-2}.$$

Thus, available optical lasers provide ξ up to 100, meanwhile with the next generation of laser systems one can manipulate with beams at $\xi > 1000$. In such ultrastrong laser fields, electrons can reach to ultrarelativistic energies. However to obtain ultrarelativistic net energies for field-free electrons one should bypass the limitations imposed by the well known Lawson-Woodward theorem [8]. One way to get net energy exchange is to use coherent processes of laser-particle interaction with the additional resonances. Among those the induced Cherenkov, Compton, and undulator processes are especially of interest [9, 10]. In these induced processes one can obtain moderate relativistic electron beams of low energy spreads and emittances due to the threshold character of nonlinear resonance in the strong wave field. Besides, the use of a plasma medium [11] is a promising

way of achieving laser-driven electron acceleration. However, laser-plasma accelerator schemes face problems connected with the inherent instabilities in laser-plasma interaction processes. The spectrum of direct acceleration mechanisms of charged particles by a single laser pulse is very restricted, since one should use the laser beams focused to subwavelength waist radii, or use subcycle laser pulses, or use radially polarized lasers. All these scenarios with different field configurations have been investigated both theoretically and experimentally [12–28]. The Lawson-Woodward theorem can also be bypassed by terminating the field, either by reflection, absorption, or diffraction [29]. The proof of principle experiment of this type has been reported in Ref. [30]. Here it is used initially relativistic electron beam and a moderately strong laser pulse. To obtain dense enough electron bunches it is reasonable to consider electrons acceleration from nanoscale-solid plasma-targets [31–34] at intensities high enough to separate all electrons from ions [35]. Thus, combining these two schemes one can obtain ultrarelativistic solid density electron bunches. Such bunches can be used to obtain high-flux of positrons, γ -quanta with possible applications in material science, medicine, and nuclear physics.

In the present work we propose an efficient mechanism for creation of ultrarelativistic field-free electron bunches, gamma-ray and positron beam of high fluxes by a single laser pulse of ultrarelativistic intensities. The scheme is as follows: a laser beam of ultrarelativistic intensities is focused onto nanoscale-solid plasma-target with relatively low Z . From this target under the action of ultrashort laser pulse a superdense electron bunch is formed and accelerated up to ultrarelativistic energies. Then we place a high- Z target (tungsten or gold) at the distances where the electron bunch gains maximum energy from the laser pulse. The purpose of the second target is twofold. First, it acts as a reflector for laser pulse, being practically transparent for electron bunch. As a consequence we get field-free ultrarelativistic electron bunch. Second, within this target with sufficiently large thickness the generation of hard γ -quanta and positron fluxes

takes place due to the electron-ion collisions.

The organization of the paper is as follows. In Sec. II for supershort strongly nonplane ultrarelativistic laser pulses of linear and circular polarizations 3D3V problem is solved via numerical simulations. In Sec. III we present numerical calculations for produced γ -quanta and positron fluxes. Finally, conclusions are given in Sec. IV.

II. GENERATION OF ULTRARELATIVISTIC ELECTRON BUNCHES FROM NANOTARGETS

Here we report on the results of the 3D3V simulations of superintense laser beam interaction with solid-plasma-targets. The illustration of proposed scheme is as follows: a laser beam of ultrarelativistic intensities ($\xi \gg 1$) is focused onto solid-plasma-target of nanothickness with relatively low \mathcal{Z} . For concreteness we take carbon target ($\mathcal{Z} = 6$). Target is assumed to be fully ionized. This is justified since the intensity for full ionization of carbon is about 10^{19} W/cm², while we use in simulations intensities at least on two order of magnitude larger. So, the target will become fully ionized before the arrival of the pulse peak. Electrons are assumed to be cold in the target, $T_e = 0$. The carbon target size is $50\lambda \times 50\lambda$ in the xy plane and $d = 0.002\lambda$ in z direction (wave propagation direction). The foil is chosen to be thin enough for the laser beam to push out all electrons from the target. In this case, only electrons are accelerated, while the ions are left unmoved. For this regime [35], the relativistic invariant parameter of the laser field ξ must be larger than the normalized field arising from electron-ion separation: $\eta = 2\pi(n_e/n_c)d/\lambda$. Here n_e is the electron density ($n_e \simeq 6.5 \times 10^{23}$ cm⁻³ for carbon) and $n_c = m\omega^2/(4\pi e^2)$ is the critical density. We assume laser radiation of $\lambda = 800$ nm and therefore $n_c \simeq 1.74 \times 10^{21}$ cm⁻³. For the chosen thickness $d = 1.6$ nm we have $\eta \simeq 4.7$. Thus, to fulfill the condition $\xi > \eta$ for all calculations we take $\xi = 20$ for a laser beam of circular polarization and $\xi = 30$ -for a linear one. Although the electron density is overcritical, the target is much thinner than the skin depth and is therefore transparent for the laser beam. Thus, from this target under the action of ultrashort laser pulse a superdense electron bunch as a thin sheath is formed and accelerated up to ultrarelativistic energies. Hence, their motion is well described in a single-particle picture, i.e. we will solve relativistic equations of motion for macroparticles

$$\frac{d\mathbf{\Pi}}{dt} = \frac{e}{mc} \left(\mathbf{E} + \frac{\mathbf{\Pi} \times \mathbf{H}}{\gamma} \right), \quad \frac{d\gamma}{dt} = \frac{e}{mc} \frac{\mathbf{\Pi} \cdot \mathbf{E}}{\gamma} \quad (1)$$

in the given electric \mathbf{E} and magnetic \mathbf{H} fields. Here we have introduced normalized momentum $\mathbf{\Pi} = \mathbf{p}/(mc)$, energy $\gamma = \sqrt{1 + \mathbf{\Pi}^2}$ (Lorentz factor) and have taken into account that charge to mass ratio of macroparticles is the same as for the electron.

The laser beam is focused at the $z = 0$ and propagates along the OZ . For analytic description of such pulses

of linear/circular polarization we will approximate corresponding electromagnetic fields as follow[36]:

$$E_x = \tilde{E}_0(\mathbf{r}, t) \left(\cos \varphi_- - \frac{z}{z_R} \sin \varphi_- \right), \quad (2)$$

$$E_y = g \tilde{E}_0(\mathbf{r}, t) \left(\sin \varphi_- + \frac{z}{z_R} \cos \varphi_- \right), \quad (3)$$

$$E_z = \frac{\tilde{E}_0(\mathbf{r}, t) \lambda}{\pi w^2(z)} \left[\left(gy \left(1 - \frac{z^2}{z_R^2} \right) - 2 \frac{zx}{z_R} \right) \cos \varphi_- + \left(x \left(1 - \frac{z^2}{z_R^2} \right) + 2g \frac{zy}{z_R} \right) \sin \varphi_- \right], \quad (4)$$

$$H_x = -E_y, \quad H_y = E_x, \quad (5)$$

$$H_z = \frac{\tilde{E}_0(\mathbf{r}, t) \lambda}{\pi w^2(z)} \left[\left(-gx \left(1 - \frac{z^2}{z_R^2} \right) - 2 \frac{zy}{z_R} \right) \cos \varphi_- + \left(y \left(1 - \frac{z^2}{z_R^2} \right) - 2g \frac{zx}{z_R} \right) \sin \varphi_- \right], \quad (6)$$

where

$$\tilde{E}_0(\mathbf{r}, t) = E_0 \frac{w_0^2}{w^2(z)} e^{-\frac{\rho^2}{w^2(z)}} f(t - z/c) \quad (7)$$

is the envelope function, g is the parameter of ellipticity; $g = 0$ corresponds to a linear polarization and $g = 1$ - circular polarization, E_0 is the electric field amplitude, $\rho^2 = x^2 + y^2$, $w(z) = w_0 \sqrt{1 + z^2/z_R^2}$, where $z_R = \pi w_0^2/\lambda$ is the Rayleigh length of the focused laser pulse with the waist w_0 in the focal plane $z = 0$, and $\varphi_- = \omega t - kz(1 + w_0^2 \rho^2 / (2z^2 w^2(z)))$ is the deformed phase. The laser pulse has temporal profile $f(t) = \cosh(t/\mathcal{T})$ with the pulse durations $\mathcal{T} = 4\lambda/c$. The carbon target is situated at $z_t = -150\lambda$. For the numerical calculations the total number of macroparticles is taken to be 4×10^4 and uniformly distributed in the target. The set of equations for the macroparticles has been solved using a standard fourth-order Runge-Kutta algorithm.

As the employed laser pulse is of nonplane configuration, here there is acceleration effect of particles even in the field of a single pulse. However, the latter is small in accordance with the above mentioned Lawson-Woodward theorem [8], to assess of which we made simulations with a single pulse given by Eqs. (2)-(6). For this setup the energy distribution in accelerated electron layer is shown in Fig. 1 for various z . Calculation have been made for the circularly polarized wave with $w_0 = 40\lambda$ and $\xi = 20$ ($I_{\max} \simeq 1.7 \times 10^{21}$ W cm⁻²). As Fig. 1 evidences, the residual acceleration because of nonplane character of a focused laser beam is small. Meantime, as is seen from

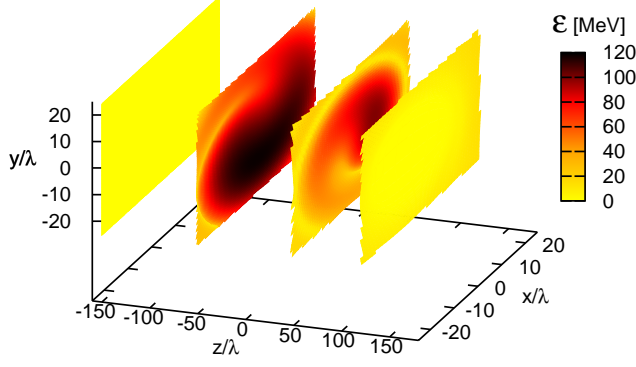


FIG. 1: (Color online) Energy distribution in accelerated electron layer is shown at various z for circularly polarized wave with $w_0 = 40\lambda$ and $\xi = 20$. There is no reflector-target.

this figure in the laser field electrons reach ultrarelativistic energies. Thus, to keep the energy gained from the wave field we propose to place a high- Z target near the position $z = z_m$ where electrons gain maximal amount of energy from the laser pulse. The purpose of the second target is twofold. First, it acts as a reflector for laser pulse, being practically transparent for electron bunch. As a consequence, we will get field-free ultrarelativistic electron bunch in the high- Z target. Second, within this target with sufficiently large thickness the generation of γ -ray and positrons take place due to the electron bunch-high- Z ion collisions. Due to high density and thickness (which should be much larger than skin depth) of second target we will consider it as a perfect reflector. Hence, one should solve the equations (1) taking into account also reflected wave. For the total electric $\mathbf{E}^{(\text{tot})}$ and magnetic $\mathbf{H}^{(\text{tot})}$ fields we will have: for $z > z_m$

$$\mathbf{E}^{(\text{tot})} = 0, \quad \mathbf{H}^{(\text{tot})} = 0 \quad (8)$$

while for $z \leq z_m$

$$E_{x,y}^{(\text{tot})}(\mathbf{r}, t) = E_{x,y}(x, y, z, t) - E_{x,y}(x, y, -z + 2z_m, t), \quad (9)$$

$$E_z^{(\text{tot})}(\mathbf{r}, t) = E_z(x, y, z, t) + E_z(x, y, -z + 2z_m, t), \quad (10)$$

$$H_{x,y}^{(\text{tot})}(\mathbf{r}, t) = H_{x,y}(x, y, z, t) + H_{x,y}(x, y, -z + 2z_m, t), \quad (11)$$

$$H_z^{(\text{tot})}(\mathbf{r}, t) = H_z(x, y, z, t) - H_z(x, y, -z + 2z_m, t). \quad (12)$$

The typical picture of acceleration dynamics is shown in Fig. 2, where energy distribution in accelerated electron layer is shown for various z for the circularly polarized wave with $w_0 = 40\lambda$. The reflector-target is situated at $z_m = 0$. As is seen from Fig. 2, after the passing the

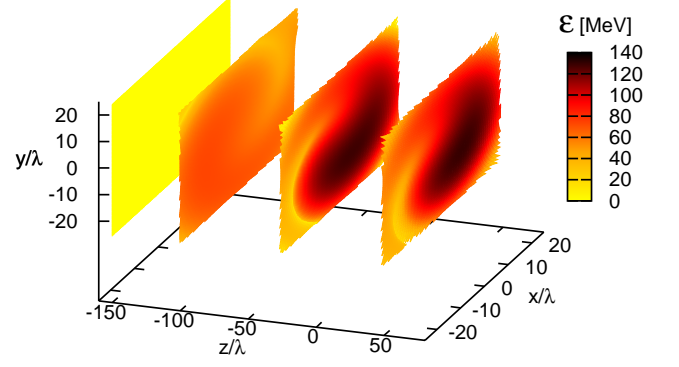


FIG. 2: (Color online) Energy distribution in accelerated electron layer is shown at various z for circularly polarized wave with $w_0 = 40\lambda$ and $\xi = 20$. Reflector-target is situated at $z_m = 0$.

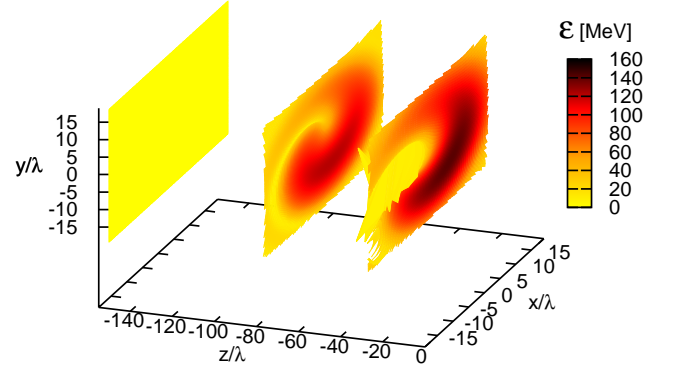


FIG. 3: (Color online) Energy distribution in accelerated electron layer at various z for circularly polarized wave with $w_0 = 15\lambda$ and $\xi = 20$. Reflector-target is situated at $z_m = -50\lambda$.

second target we have field-free ultrarelativistic electron bunch.

For the smaller waists w_0 the position of energy maximum takes place for the smaller interaction lengths $|z_t - z_m|$. In Fig. 3, we represent the results for circularly polarized wave with $w_0 = 15\lambda$ and $\xi = 20$. For this setup the reflector-target is situated at $z_m = -50\lambda$. We have made calculations also for the linearly polarized laser beam. In Fig. 4, the results for linearly polarized laser beam ($g = 0$) with $w_0 = 10\lambda$ and $\xi = 30$ ($I_{\text{max}} \simeq 1.9 \times 10^{21} \text{ W cm}^{-2}$) are presented. As is seen from this figure, in the field-free region we have an ultrarelativistic electron bunch of energies $\sim 200 \text{ MeV}$.

Note that in the high- Z target due to the electron

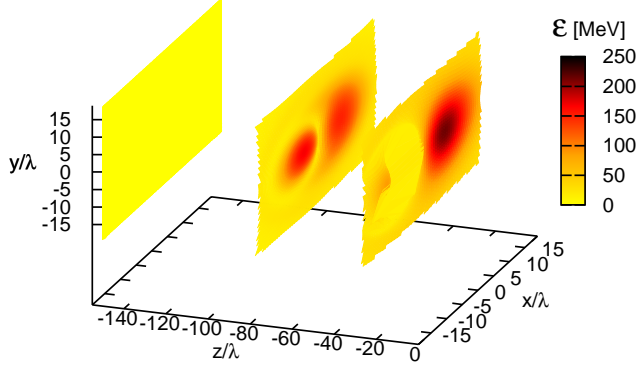


FIG. 4: (Color online) Energy distribution in accelerated electron layer at various z for linearly polarized wave with $w_0 = 10\lambda$ and $\xi = 30$. Reflector-target is situated at $z_m = -50\lambda$.

bunch-ion collisions the electrons will lose energy via the generation of γ -quanta and positrons. Hence, if one expects to obtain unperturbed electron bunch, the target thickness should be much smaller than the radiation length, otherwise along with primary bunch one will have substantial amounts of produced gamma-ray photons and positrons. This scenario is also of interest and will be considered in the next section.

III. PRODUCTION OF HARD γ -QUANTA AND POSITRONS WITH LASER GENERATED ULTRARELATIVISTIC ELECTRON BUNCHES

As is seen from the figures 1-4, the energy distribution of accelerated electrons obtained by the laser-target interaction is usually broad with almost 100% energy spread up to a cutoff energy. Such electron bunches are not suitable for coherent effects, for example, to generate coherent radiation -free electron laser. However, such bunches of high energy-density can be used to obtain high-flux of positrons, hard γ -quanta with possible applications in material science, medicine, and nuclear physics. Note that in our scheme this can be implemented by all-optical means without use of large scale facilities such as nuclear reactors or conventional particle accelerators. One can use second target as a bremsstrahlung converter, leading to the emission of bremsstrahlung photons, the energy of which takes a maximum value equal to that of the accelerated electrons. Then, the bremsstrahlung photons interacting with ions can produce electron-positron pairs. In other words, QED cascade can be developed. Accurate calculations of γ -quanta and positrons spectra in such targets require using Monte Carlo computer codes (see, e.g., Ref. [37] and references therein). However, one can use relatively simple formulas [38] for thin targets, when

target thickness is smaller than the radiation length \mathcal{L}_{rad} :

$$\mathcal{L}_{\text{rad}} = \left(4\alpha N_i \mathcal{Z}^2 r_0^2 \log \frac{183}{\mathcal{Z}^{1/3}} \right)^{-1}, \quad (13)$$

where $\alpha = e^2/\hbar c = 1/137$ is the fine structure constant, N_i is the density of ions, r_0 - is the electron classical radius. In particular, for gold ($\mathcal{Z} = 79$, $N_i = 5.9 \times 10^{22} \text{ cm}^{-3}$) $\mathcal{L}_{\text{rad}} \simeq 0.31 \text{ cm}$, and for tantalum ($\mathcal{Z} = 73$, $N_i = 5.55 \times 10^{22} \text{ cm}^{-3}$) $\mathcal{L}_{\text{rad}} \simeq 0.39 \text{ cm}$. Thus, the γ -quanta number distribution N_γ over energy ε_γ obeys integro-differential equation [38]:

$$\frac{\partial N_\gamma(\varepsilon_\gamma, \zeta)}{\partial \zeta} = \int_0^1 N_e\left(\frac{\varepsilon_\gamma}{v}, \zeta\right) \varphi_0(v) \frac{dv}{v} - \sigma_0 N_\gamma(\varepsilon_\gamma, \zeta), \quad (14)$$

Here $\sigma_0 \simeq 7/9$, and $\varphi_0(v)$ describes bremsstrahlung process, which in the case of complete screening is given by the formula:

$$\varphi_0(v) = \frac{1}{v} \left(1 + (1-v)^2 - \varkappa_0(1-v) \right), \quad (15)$$

where $\varkappa_0 \simeq 0.64$. The quantity ζ in Eq. (14) is the target thickness measured in radiation lengths, $N_e(\mathcal{E}, \zeta)$ is the electron/positron distribution function, that should be defined self-consistently. However, for small ζ , in Eq. (14) we take $N_e(\mathcal{E}, \zeta) = N_e(\mathcal{E}, 0)$, where $N_e(\mathcal{E}, 0)$ is the distribution function at the entrance to high- \mathcal{Z} target. Thus, for small ζ we have

$$N_\gamma(\varepsilon_\gamma, \zeta) \simeq \zeta \int_0^1 N_e\left(\frac{\varepsilon_\gamma}{v}, 0\right) \varphi_0(v) \frac{dv}{v}. \quad (16)$$

In the limit of low annihilation rates the positrons distribution function can be defined as

$$\frac{\partial N_{e+}(\mathcal{E}, \zeta)}{\partial \zeta} = \int_0^1 N_\gamma\left(\frac{\mathcal{E}}{u}, \zeta\right) \psi_0(u) \frac{du}{u}, \quad (17)$$

where $\psi_0(u)$ describe pair production process, which in the case of complete screening is given by the formula [38]:

$$\psi_0(u) = u^2 + (1-u)^2 + \varkappa_0 u(1-u). \quad (18)$$

Thus, having at hand electron bunch distribution $N_e(\mathcal{E}, 0)$ with the help of Eqs. (16) and (17) one can calculate hard γ -quanta and positrons number distribution over energy. For the target thickness we take $\zeta = 0.2$. We have made calculations for the setup of figures 3 and 4. To obtain electron bunch distribution $N_e(\mathcal{E}, 0)$ at the entrance to bremsstrahlung target we considered the effective area limited to the central zone between $-20\lambda < x, y < 20\lambda$. The results of calculations are presented in Figs 5 and 6. In these figures, in the logarithmic scale it is shown the energy distribution functions for

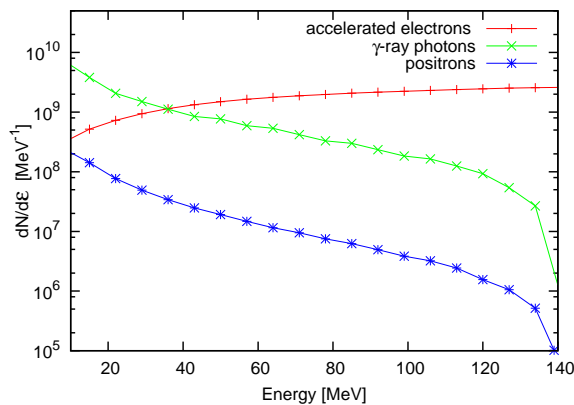


FIG. 5: (Color online) In the logarithmic scale it is shown the energy distribution functions for primary accelerated electrons, produced γ -quanta and positrons for the setup of Fig. 3.

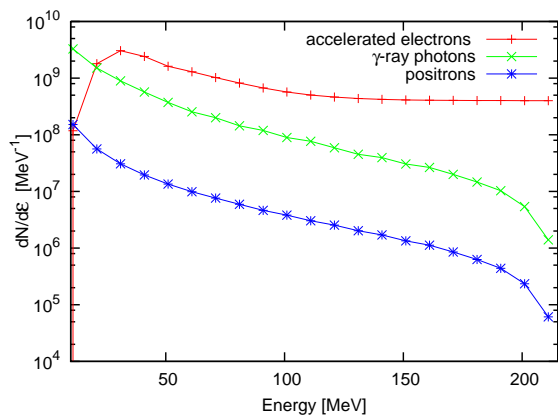


FIG. 6: (Color online) Same as Fig. 5, but for the setup of Fig. 4.

primary accelerated electrons, produced γ -quanta, and positrons. As is seen from these figures, through two-target scheme one can produce dense electron/positron bunches and substantial amounts of γ -quanta of energies up to 200 MeV. In particular, for Fig. 6 the number of photons in the range of 50 – 200 MeV is $\sim 10^9$.

IV. CONCLUSION

We have proposed mechanism for generation of high energy-density particles bunches from nanotargets by single laser pulse of ultrarelativistic intensities. We consider two target scheme where one ultrathin target serve as a source of dense electron bunch. The purpose of the second target is twofold. First, it acts as a reflector for laser pulse, thus abruptly terminating the wave field and therefore allows electrons to keep the gained from the wave energy. Second, within this target with sufficiently large thickness the intensive generation of hard γ -quanta and positrons occurs due to the electron-ion collisions. In particular, the considered setup provides generation of high energy-density positrons and γ -quanta that may have applications in material science, medicine, and nuclear physics.

Acknowledgments

This work was supported by SCS of RA.

-
- [1] V. Yanovsky, *et al.*, Opt. Express **16**, 2109 (2008).
 - [2] J. H. Sung, S. K. Lee, T. J. Yu, T.M. Jeong, and J. Lee, Opt. Lett. **35**, 3021 (2010).
 - [3] A.V. Korzhimanov, A. A. Gonoskov, E.A. Khazanov, A. M. Sergeev, Phys. Usp. **54**, 9 (2011).
 - [4] Z. Wang, C. Liu, Z. Shen, Q. Zhang, H. Teng, Z. Wei, Opt. Lett. **36**, 3194 (2011).
 - [5] The Extreme Light Infrastructure (ELI) project: <http://www.extreme-light-infrastructure.eu/eli-home.php>
 - [6] Exawatt Center for Extreme Light Studies: <http://www.xcels.iapras.ru>
 - [7] High Power laser Energy Research: <http://www.hiper-laser.org>
 - [8] P.M. Woodward, J. Inst. Electr. Eng. **93**, 1554 (1947); J.D. Lawson, IEEE Trans. Nucl. Sci. **26**, 4217 (1979).
 - [9] H.K. Avetissian, *Relativistic Nonlinear Electrodynamics* (Springer, New York, 2006).
 - [10] H. K. Avetissian, S. S. Israelyan, Kh. V. Sedrakian, Phys. Rev. ST AB **10**, 071301 (2007); H. K. Avetissian, Kh. V. Sedrakian, *ibid.* **13**, 101304 (2010); *ibid.* **13**, 081301 (2010).
 - [11] E. Esarey, C. B. Schroeder, W. P. Leemans, Rev. Mod. Phys. **81**, 1229 (2009).
 - [12] E. Esarey, P. Sprangle, J. Krall, Phys. Rev. E **52**, 5443 (1995).
 - [13] F. V. Hartemann, S. N. Fochs, N. C. Luhmann, J. G. Woodworth, M. D. Perry, Y. J. Chen, A. K. Kerman, A. K. Kerman, G. P. Le Sage, Phys. Rev. E **51**, 4833 (1995).
 - [14] Y. C. Huang, D. Zheng, W. M. Tulloch, R. L. Byer, Appl. Phys. Lett. **68**, 753 (1996).
 - [15] G. Malka, E. Lefebvre, J. L. Miquel, Phys. Rev. Lett. **78**, 3314 (1997).
 - [16] B. Quesnel, P. Mora, Phys. Rev. E **58**, 3719 (1998).
 - [17] G. V. Stupakov, M. S. Zolotarev, Phys. Rev. Lett. **86**, 5274 (2001).
 - [18] W. D. Kimura *et al.*, Phys. Rev. Lett. **86**, 4041 (2001).
 - [19] P. X. Wang, Y. K. Ho, X. Q. Yuan, Q. Kong, N. Cao, A. M. Sessler, E. Esarey, and Y. Nishida, Appl. Phys. Lett. **78**, 2253 (2001).
 - [20] Y. I. Salamin, C. H. Keitel, Phys. Rev. Lett. **88**, 095005 (2002).

- (2002).
- [21] S. X. Hu, A. F. Starace, Phys. Rev. Lett. **88**, 245003 (2002).
 - [22] T. Plettner, R. L. Byer, E. Colby, B. Cowan, C. M. S. Sears, J. E. Spencer, R. H. Siemann, Phys. Rev. Lett. **95**, 134801 (2005).
 - [23] C. Varin, M. Piché, M. A. Porras, Phys. Rev. E **71**, 026603 (2005).
 - [24] Y. I. Salamin, Phys. Rev. A **73**, 043402 (2006); Y. I. Salamin, Opt. Lett. **32**, 90 (2007).
 - [25] A. Karmakar, A. Pukhov, Laser Part. Beams **25**, 371 (2007).
 - [26] P.-L. Fortin, M. Piché, C. Varin, J. Phys. At. Mol. Opt. Phys. **43**, 025401 (2010).
 - [27] L. J. Wong, F. X. Kärtner, Optics Express **18**, 25035 (2010).
 - [28] F. Terranova, Phys. Rev. ST Accel. Beams **17**, 071301 (2014).
 - [29] J. A. Edinghofer, R. H. Pantell, J. Appl. Phys. **50**, 6120 (1979).
 - [30] T. Plettner, R. L. Byer, E. Colby, B. Cowan, C. M. S. Sears, J. E. Spencer, R. H. Siemann, Phys. Rev. Lett. **95**, 134801 (2005).
 - [31] Yu.M. Mikhailova, V.T. Platonenko, S.G. Rykovanov, JETP Lett. **81**, 571 (2005).
 - [32] A.S. Pirozhkov, S.V. Bulanov, T.Zh. Esirkepov, M. Mori, A. Sagisaka, H. Daido, Phys. Plasmas **13**, 013107 (2006).
 - [33] S.G. Rykovanov, J. Schreiber, J. Meyer-ter-Vehn, New J. Phys. **10**, 113005 (2008).
 - [34] H.-C. Wu, J. Meyer-ter-Vehn, J. Fernández, B. M. Hegelich, Phys. Rev. Lett. **104**, 234801 (2010).
 - [35] V.V. Kulagin, V.A. Cherepenin, M.S. Hur, H. Suk, Phys. Rev. Lett. **99**, 124801 (2007).
 - [36] K. T. McDonald, arXiv:physics/0003056v2
 - [37] S. Agostinelli et al, Nucl. Instrum. Methods Phys. Res. A **506**, 250 (2003).
 - [38] B. Rossi, K. Greisen, Rev. Mod. Phys. **13**, 240 (1941).